Available online at www.sciencedirect.com

jmr&t Journal of Materials Research and Technology

journal homepage: www.elsevier.com/locate/jmrt

Original Article

Strategized friction stir welded AA6061-T6/SiC composite lap joint suitable for sheet metal applications

Suresh S [a,*], *Elango Natarajan* [b,e], *Ragavanantham Shanmugam* [c], *Venkatesan K* [d], *Saravanakumar N* [e], *AntoDilip A* [e]

[a] *Department of Mechanical Engineering, Muthayammal Engineering College, India*
[b] *Faculty of Engineering, Technology and Built Environment, UCSI University, Kuala Lumpur, Malaysia*
[c] *Advanced Manufacturing Engineering Technology, School of Engineering, Math and Technology, Navajo Technical University, Crown Point, NM 87313, USA*
[d] *Department of Metallurgical Engineering, Government College of Engineering, Salem, India*
[e] *Department of Mechanical Engineering, PSG Institute of Technology and Applied Research, Coimbatore, India*

ARTICLE INFO

Article history:
Received 5 August 2022
Accepted 6 September 2022
Available online 13 September 2022

Keywords:
FSW
AA6061-T6
SiC
Nanoparticles
Microhardness

ABSTRACT

Friction Stir Welding (FSW) is one of the best choices of joining light weight metal structures involving lap joints as conventional welding methods find difficult in getting sound weld joints. Aluminium alloys are lightweight materials relatively used in space frame structures, ship buildings and panels of automotive vehicles. Main objective of this research is to investigate Al–SiC FSW lap joints and to examine the suitable pre-fill nanoparticles in the configured grooves to augment the weld strength. Three different volume additions of SiC nanoparticles and tool rotational speed were considered to fabricate lap joints for the investigations. Tool rotational speed and volume of SiC reinforcement have a significant impact on the dissemination of SiC in the weldment and weld quality. The spread of SiC nanoparticles in the weld area strongly affects the weld microstructure and mechanical characteristics. Nano SiC filled lap joint has shown a significant improvement in mechanical properties as compared to a joint without nanoparticles. The best lap joint is achieved with 20 vol% of SiC and 1500 rpm of rotational speed. The investigations imply that the tensile strength is decreased for joints with 26 vol% of SiC, due to clustering of reinforcement particles. The supplement of SiC nanoparticles restricts the growth of grains and refines the stir zone (SZ) microstructure and hence this method of weld process is recommended for lap weld joints in metal structures.

* Corresponding author.
E-mail address: suresh.mjl@gmail.com (S. S).

https://doi.org/10.1016/j.jmrt.2022.09.022

1. Introduction

Investigation of lightweight materials and extensive use of such materials in various applications, especially in automotive and aerospace body structure applications [1,2] is seen in recent decades. The most commonly used commercial lightweight structural material is aluminium alloys [3]. It is one of the material complies with European Environmental Protection Directives: 2000/53/CE-ELV for the automotive sector and meet the sustainable development goals (SDGs) [4]. However, the joining of aluminium alloy parts by fusion based welding results low weld strength especially in the heat-affected zone (HAZ) due to high heat generation [5]. FSW is a prevalent welding process where the base materials are heated below the crystallization temperature and hence affords a better alternative to overcome the problems in infusion joining process [6,7]. Some special attention is required in joining thin Al alloy sheets to avoid issue like sheet wrapping, which needs low heat input and special fixture [8,9]. Besides, the thin sheet FSW joint comprises different microstructure and mechanical properties due to heat loss and insufficient material flow [10,11]. Though tool rotational speed, tool feed rate, shoulder plunge depth, and tool profile are the process parameters determining the quality of the weld joint in the FSW process [12], tool rotational speed plays an important role in preparing sound joints as compared to other process parameters [13–16].

Adding ceramic particles between the abutting surfaces during friction stir welding (FSW), friction stir processing (FSP) and friction stir spot welding (FSSW) has received rising attention in past few decades [17–23]. Jafari et al. [24] examined the distribution of residual stress in SiC incorporated Al alloy. They reported that the incorporation of the SiC has a considerable influence on the residual stress distribution. Singh A et al. [25] examined the FSW on Zn interlayer AA6061 joints and reported that Zn interlayer joints show equivalent tensile strength, but higher hardness (about 60%) than Zn free joints. Singh et al. [26] revealed the impact of Al_2O_3 reinforcement in AA6061 butt joints and reported that the higher rotational speed (2000 rpm) would provide the homogeneous distribution of Al_2O_3 in the weld region and would achieve maximum weld strength of 250 MPa. Bahrami et al. [27] investigated the FSW of AA7075-O butt joint with reinforcing SiC nanoparticles and found that the reinforcement considerably influenced the weld strength. It was also shown that the presence of SiC in the grain boundaries prevents grains growth. In addition, the increased tool rotation speed makes the dispersion of nanoparticles uniform in the welding area. Rita Maurya et al. [28] used carbon nanotubes to produce an MMC layer in AA6061 by Friction Stir Processing (FSP) and reported that the fabricated MMC surface composite has greater mechanical properties compared to the base metal because of microstructural modification.

Naturally, the weld strength may be affected by agglomeration or coarsening of reinforced particles during FSW or FSP. Babu et al. [26] observed that agglomerated fillers considerably reduce the joint strength and hardness of Oxide Dispersion Strengthened (ODS) nickel-based metal matrix composite joint. The slight coarsening of reinforcement particles in FSW may affect the hardness of the composite joint as reported by West et al. [29]. It is manifested that the addition of finely dispersed ceramic nanoparticles in weld region would improve weld properties. The challenge of agglomeration in reinforcement is open ended and needed to be investigated.

The influence of the addition and distribution of the SiC nanoparticles in various zones of FSW AA6061-T6 joints in lap configuration has not been attempted and presented so far. In the current investigations, FSW lap joints were done on Al 6061-T6 alloy sheet with the proposed reinforcement deposition strategy to produce composite joint. The suitable volume fraction of fillers and operating condition that presents the best weld joints was investigated, analysed, and reported.

2. Materials and methods

US ASTM AISI and SAE Standards 6061 Aluminium Alloy 6061-T6 sheets of 100 mm × 100 mm × 2 mm and SiC nanoparticle fillers of 50 nm in diameter were used for lap weld joints. Al 6061-T6 alloy has aluminium with Mg of 0.708%, Si of 0.43%, and Fe of 0.49% as major constituents and Cu of 0.164%, Cr of 0.14%, Mn of 0.097%, Ti of 0.04%, Zn of 0.004% as minor constituents. It has good machinability and toughness because of higher percentage of Mg and Si. Al sheet samples were fabricated in-house by stir casting method. The weld tool is hardened H13 steel with 55–60 HRC that has better wear resistance. It has shoulder diameter of 12 mm, threaded pin diameter of 5 mm, and pin length of 3 mm.

The volume of SiC nanoparticles and tool rotational speed were considered as varying process parameters in the current investigations. To perform welding, sheets were overlapped by 35 × 100 mm and SiC nanoparticles were added into the rectangular slot at overlapped section as shown in Fig. 1(a). The SiC nanoparticle was packed tightly in the slot and the slot was closed by passing the pin less tool having a shoulder diameter of 12 mm to restrict the spill out of the packed particles during the FSW process. The photograph of the closed portion of the SiC packed slot is shown in Fig. 1(b).

Width of the rectangular slot was changed as 1.0, 1.5, and 2 mm while keeping constant depth of the slot to accommodate the different volume fraction of SiC nanoparticles. The volume fraction of SiC nanoparticles was calculated based on the slot dimensions and the tool pin dimensions [30].

$$\text{Theoretical Volume Fraction } (v_t) = \frac{\text{Area of Groove}}{\text{Projected Area of Tool Pin}} \quad (1)$$

Three different volume fractions of SiC nanoparticles viz. 13%, 20% and 26% and three different tool rotational speed viz. 1200 rpm, 1500 rpm and 1800 rpm were used. The embedded condition of process parameters is mentioned in Table 1. The other process parameters such as tool feed rate of 20 mm/min, tool tilt of 0°, and a shoulder plunge depth of 0.2 mm were kept constant. The weld parameters were chosen based on the preliminary studies and the existing literatures [8,10,31].

All weld samples were prepared with a help of specially made fixture attached to the CNC vertical machining center. Samples for lap shear tensile test, microhardness test and

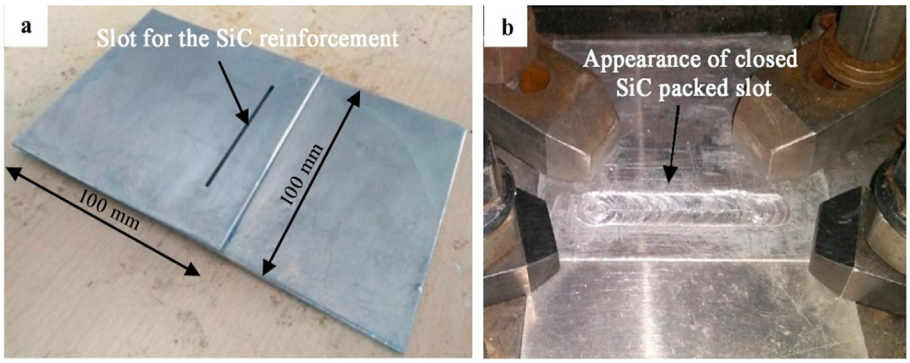

Fig. 1 – (a) Position of the slot for nanoparticles reinforcement (b) SiC packed slot is closed by a pinless tool to avoid the spill out of the packed SiC during tool travel.

metallurgical examinations were prepared using the wire-EDM from the welded samples. Lap shear tensile tests were conducted at 1 mm/min and at room temperature as per ANSI/AWS/SAE/D8.9-97. Computerized universal testing machine (Make: TE-JINAN-WDW100) was used to record load–displacement data [32]. Micro hardness across the weld joints were measured using Vickers microhardness tester by applying 150 g of load for 30 s. Until otherwise stated, three repeat specimens were used to certain the repeatability of the tests.

To study microstructure and its allied characteristics, the specimens were polished using conventional polishing method then etched with Keller's regents for 20 s. The microstructure of the weld cross-section and fractured surface of lap shear tested samples were characterized using Optical Microscope (OM: Invertoplan TR) and Field Emission Scanning Electron Microscope (FESEM: SIGMA-Carl Zeiss). X-ray Diffraction (XRD: X'Pert^3 Powder) was used to evaluate the formation of phases in the stir zone.

3. Results and discussion

3.1. *Weld structure characterization*

Fig. 2 displays macrographs of upper surface of the samples that were prepared at different volume fraction of SiC and at different welding speeds.

Table 1 – Weld plan and its respective sample code.

Sl. No.	Volume Fraction of SiC (VF) (%)	Tool rotational speed (N) (rpm)	Sample code
1	13	1200	13–1200
2	13	1500	13–1500
3	13	1800	13–1800
4	20	1200	20–1200
5	20	1500	20–1500
6	20	1800	20–1800
7	26	1200	26–1200
8	26	1500	26–1500
9	26	1800	26–1800

There is no defect apparently observed on the weld joints. Besides, more flash is noticed in the advancing side (AS) as the tool rotational speed was increased irrespective of the volume fraction of SiC. Undersized insufficient filling of the stirring materials is observed at samples with 26 vol% of SiC due to insufficient stirring of SiC. It is concluded from the investigations that higher volume fraction of SiC above 26 vol% is not advisable. Homogeneous welding seam is observed in almost all samples. The welding is seen very stable at the tool rotational speed of less than 1800 rpm, except that the slight flashier is found on the retreating side of some joints. More flash is generated at a high rotational speed or higher volume percentage of SiC.

Fig. 3 depicts the macrograph of cross-sectioned FSW lap joints, that were prepared under different welding conditions. The macrostructures reveal the entire stir zone (SZ) of the joint.

It shows a bright and dark round flow pattern, which was attributed probably by the mixing of aluminium matrix and SiC nanoparticles. The stirring action initiated an interaction between the reinforced SiC nanoparticles and Al alloy during transverse movement of the tool and resulted a plasticized Aluminum/SiC composite in stir zone. Two kinds of mixing regions are roughly identified among the weld samples. (a) Particles in light region, which mostly identified in the samples with low volume fraction of SiC. (b) Particles in rich regionas as indicated in Fig. 3. The high loading of the SiC nanoparticles resulted more particles in rich region and a smaller number of particles in light region.

In general, defects are formed in FSW joints because of improper material flow and/or insufficient heat generation in the nugget zone. The various defects are pinhole, kissing bond, tunnel defect, cracks, etc. All welded joints at lower welding speed have exhibited a good appearance and free of macro-scale defects as shown in Fig. 3. A severe tunnel-like defect is found on the advancing side of samples prepared at higher welding speed (1800 rpm) as shown in Fig. 3. This defect was caused by insufficient heat input and insufficient vertical flow of plasticized material [33].

3.2. *Microstructure analysis*

Base Metal (BM), Heat-Affected Zone (HAZ), Thermo-Mechanically Affected Zone (TMAZ), and Stir Zone (SZ) at

Vol. Fraction of SiC (%)	Tool rotational speed (rpm)	Weld surface appearance	Observation
13 %	1200		Smooth weld surface
	1500		Smooth weld surface
	1800		Smooth weld surface with lateral flash
20 %	1200		Smooth weld surface
	1500		Smooth weld surface with lateral flash
	1800		Smooth weld surface with lateral flash
26 %	1200		Smooth weld surface
	1500		Weld surface with lateral flash and insufficient filling
	1800		Weld surface with lateral flash and insufficient filling

Fig. 2 – Top surface macrograph of Lap-FSW joints.

cross-section of 20–1500 (20 vol%, 1500 rpm) and 26–1500 (26 vol%, 1500 rpm) samples are shown in Figs. 4 and 5. Smaller grain size at SZ is seen because of presence of nanoparticles and severe plastic deformation in the SZ. Besides, the frictional heat and stirring action in SZ has also stretched nanoparticles and led to significant grain refinement [34].

TMAZ showed better grain refinement due to plastic deformation at high temperature, compared with BM. The observed onion ring features that contain dark and bright rings reveal the concentric distribution of SiC nanoparticles in SZ. However, darker regions are observed in samples of 26–1500 (26 vol%, 1500 rpm) as shown in Fig. 5. The improper

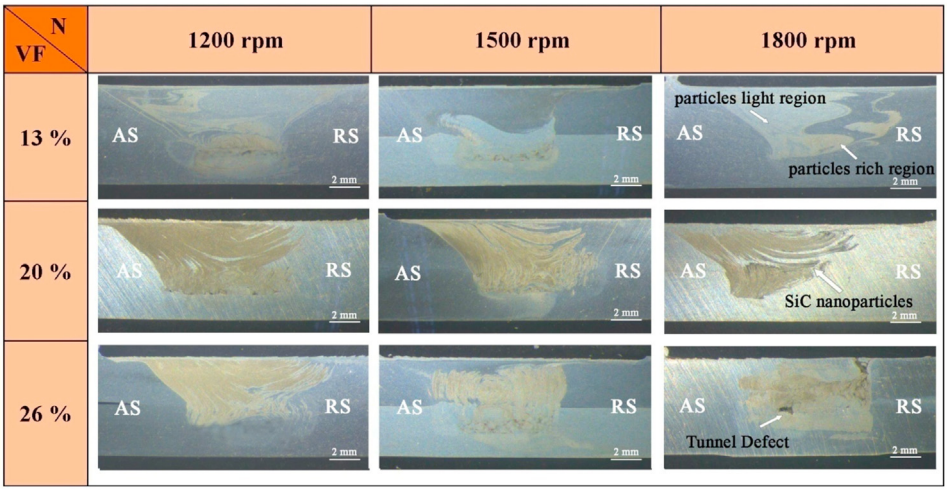

Fig. 3 – Cross-sectional structures of Lap-FSW joints at different weld condition.

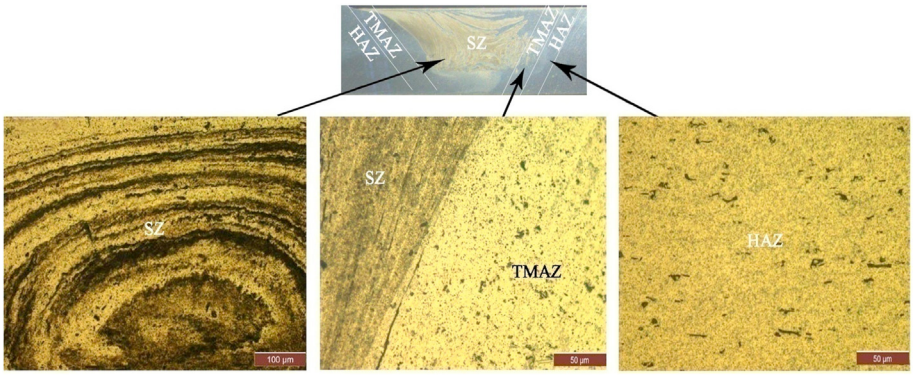

Fig. 4 – Macrographs representing SZ, SZ/TMAZ and HAZ of cross sectioned sample 20–1500.

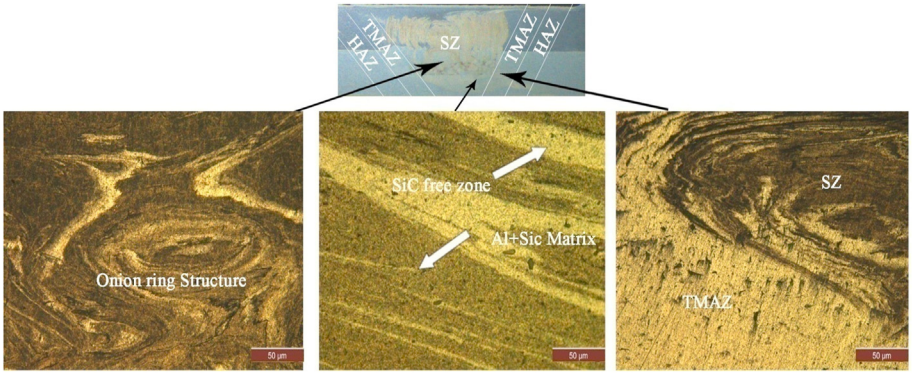

Fig. 5 – Macrographs representing SZ, SZ/TMAZ and HAZ of cross sectioned sample 26–1500.

material flow and higher volume percentage of SiC could result in localized accumulation of particles in the region [23,30].

The FESEM micrograph of SZ in sample code 20–1500 (20 vol%, 1500 rpm) is shown in Fig. 6. It can be noted that the onion ring structure in SZ is more evident in the distribution of

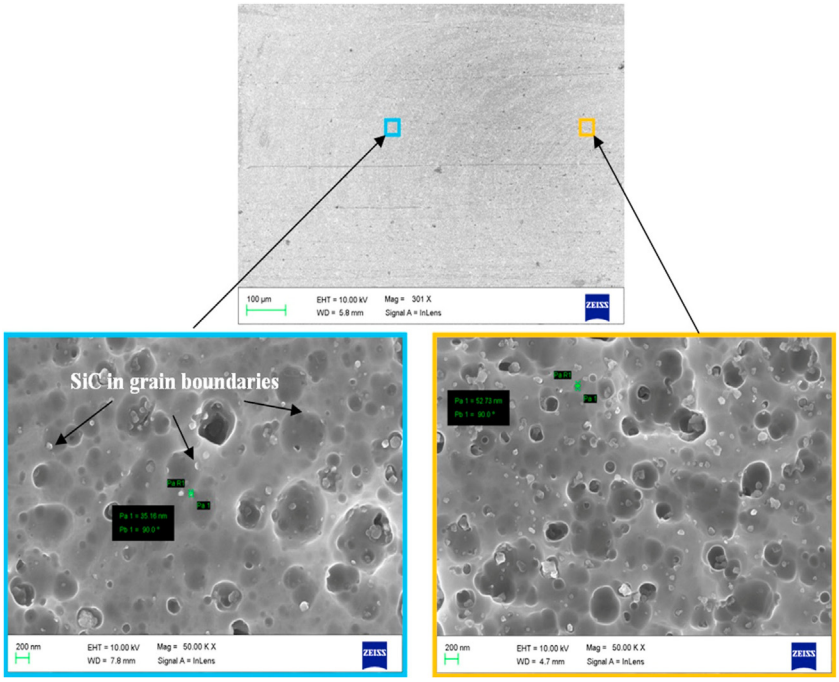

Fig. 6 – FESEM images of SZ of sample 20–1500.

SiC nanoparticles. This is attributed by the material flow during the FSW process. However, it is implied from highly magnified FESEM image that SiC nanoparticles are homogeneously distributed and evidently visible in the SZ. Besides, SiC particles had excellent cohesion with Al matrix in the grain boundaries.

Investigations clearly revealed that the SiC particles are stacked in the grain boundaries and prevented grain growth. This could be one of the reasons for the higher lap shear strength. Interestingly, the grain size of SZ in SiC reinforced weld is smaller than the grain size of SZ in SiC particles free weld. This is because of grain boundary pinning attributed by SiC nanoparticles. Besides, other reason is the severe plastic deformation in the stir zone, as well as continual dynamic recrystallization [35,36].

The FESEM micrograph of the SZ in sample code 26–1500 weld (26 vol%, 1500 rpm) is shown in Fig. 7. It shows SiC nanoparticle agglomeration at SZ, which was strongly bonded with spherical nanoparticles as indicated by arrows. More agglomeration of SiC particles could increase the interface area between aluminum matrix and SiC particles and show the poor bonding between them [2,20,37]. The presence of micro voids is also observed around SiC particles that affected mechanical property.

It is observed from the microstructure analysis that SiC incorporated weld has enhanced mechanical characteristics, when nanoparticle distribution is homogeneous in the weld area. The agglomeration of nanoparticles was occurred only at higher loading of SiC. Nanoparticle agglomeration in SZ is due to inappropriate coherence. Agglomerated nanoparticles (doubled in size) were observed in some samples like 26–1500 sample shown in Fig. 7 that has lower weld strength. The distribution of SiC in lap-FSW sample with 20 vol% is more uniform compared to the sample with 13 vol% and 26 vol%.

Fig. 8 illustrates the XRD results of Al6061-20 vol% SiC and Al6061-26 %vol SiC nano composite joints. Different peak intensities, as seen in Fig. 8, confirm the presence of aluminium and SiC particles. The presence of major peaks indicates aluminum, and minor peaks represent the SiC particles [23,38]. There is also no indication of new phases (Intermetallic Compounds), which implies to the absence of interfacial reactions and good dispersion of SiC nanoparticles during the FSW process. It can also be seen that as the volume percent of SiC is increased, the Al peaks shift somewhat to higher angles.

3.3. *Weld strength*

The measured lap shear strength of AA6061-T6/SiC lap joints is shown in Fig. 9. The welds made with a 20% volume fraction of SiC show the highest lap shear strength for all three rotational speeds. It is due to grain refinement in the nugget zone. It is also remarked that the tool rotational speed of 1500 rpm shows higher lap shear strength for all the volume fractions of SiC as compared to the other two rotational speeds.

The lap shear strength of the weld made with a 20 vol% and a tool rotational speed of 1500 rpm is 137 MPa, which is 20% greater than the lap shear strength of the weld made without SiC. The incorporation of SiC nanoparticles initiates pining effect which lead for grain refinement during FSW process. Also, addition of SiC restricts the dislocation motion.

The slot width of 1.5 mm (20 vol% SiC) and below is reported to be increased, while beyond this produce lower strength. The reason for lower strength is fact that higher amount of SiC addition leads to agglomeration or clustering, and weaker cohesion between the Al matrix and SiC particles

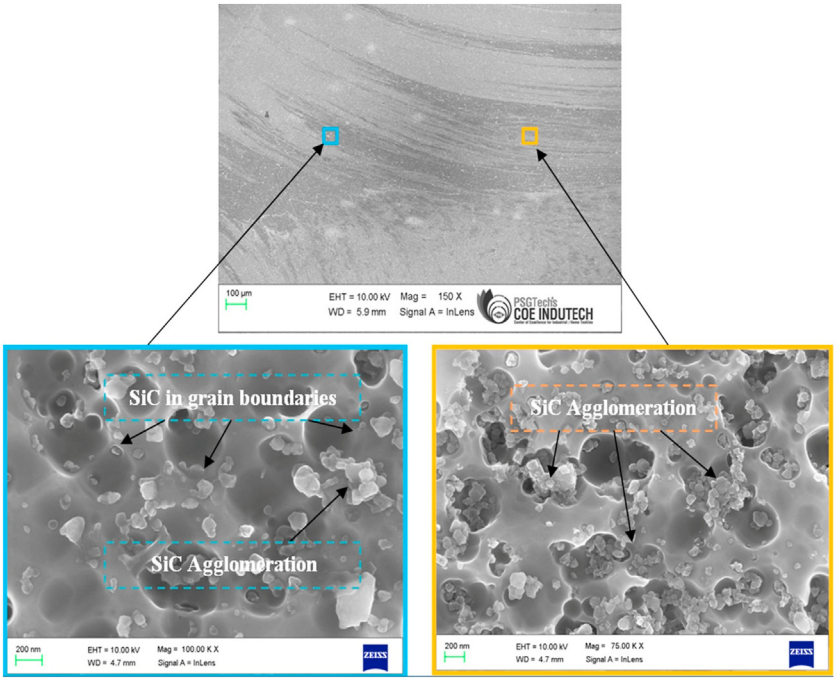

Fig. 7 – FESEM images of SZ of sample 26–1500.

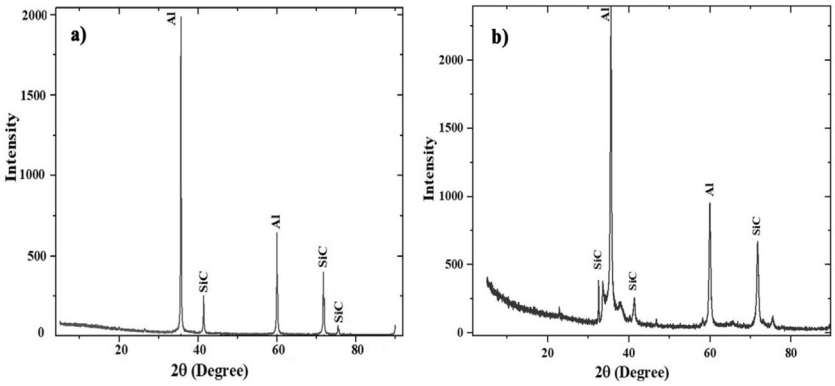

Fig. 8 – XRD of (a) 20–1500 sample, and (b) 26–1500 sample.

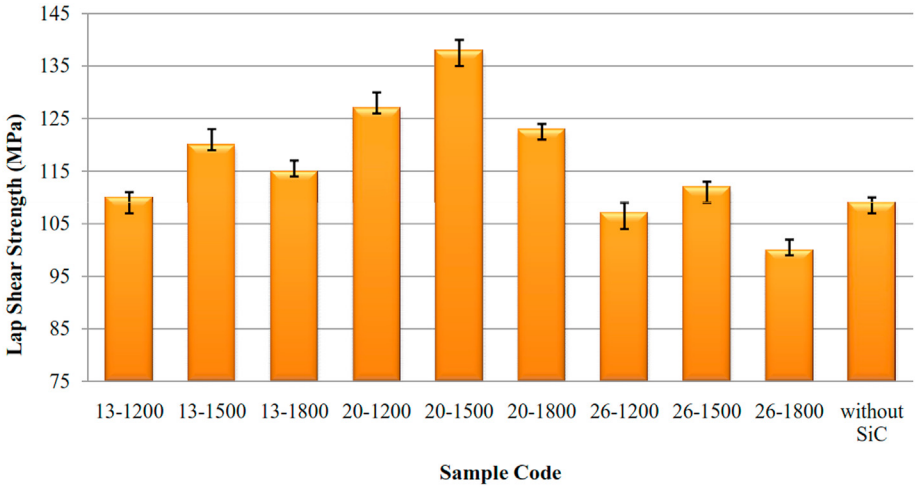

Fig. 9 – Lap Shear Strength of FSW lap joints.

as evidenced in Fig. 7. This finding is in line with findings of Anil Kumar et al. [39].

Fig. 10 depicts fractography of fractured surface of lap shear tested specimens. The images show that 20–1500 (20 vol %, 1500 rpm) specimen has failed in HAZ, while 26–1500 (26 vol%, 1500 rpm) sample has failed in SZ. FESEM micrograph of 20–1500 sample is coved with equiaxed large and deep dimples suggesting ductile fracture along with the higher elongation. This is because of fine dispersion of nanosized SiC particles in the Al matrix, which has given more resistance against deformation. However, the lack of dimples is observed in 26–1500 (20 vol% and 1500 rpm) specimen and hence no major elongation and brittle fracture is evidenced [2,40]. Moreover, fracture right from the SZ is occurred because of

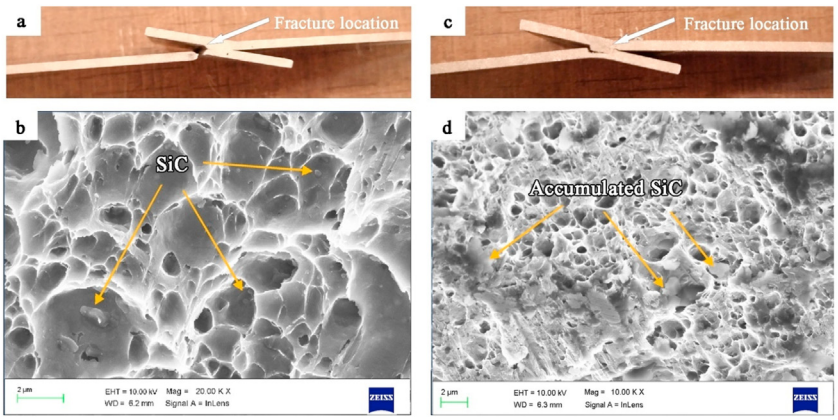

Fig. 10 – Fracture sample after tensile test and FESEM of fracture surface of sample (a–b) 20–1500 (c–d) 26–1500.

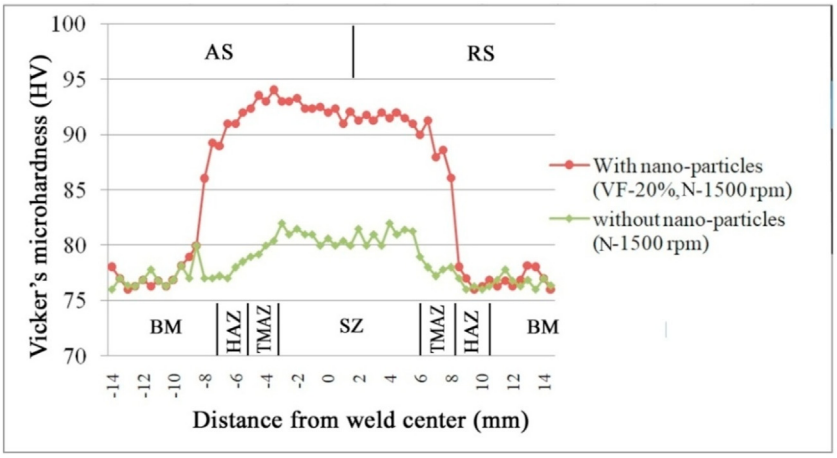

Fig. 11 – Microhardness survey of the samples with and without nanoparticles addition.

voids. In other words, the accumulated SiC particles (Fig. 10(d)) converge into small voids and lead to failure around this area. It is probably that the agglomerated particles caused by improper distribution acts as a crack nucleation sites, leading to poor lap shear strength. The accumulation of the SiC particles is responsible for premature fracture of high loaded weld samples. This result is in line with the results published by Tanvir Singh et al. [26] on FSW of 6061 with the addition of Al_2O_3.

3.4. *Microhardness of the weld*

The microhardness observed at various weld regions of 20–1500 sample and SiC-free weld sample are presented in Fig. 11. For the uniformity, both of these joints were made at 1500 rpm. The regions comprise SZ, TMAZ, HAZ and BM. The SZ of the weld made with SiC nanoparticles shows significant improvement in microhardness values as compared to SiC particles-free welds. The high plastic deformation and finer grains influence hardness of welds joints based on the Hall-Petch equation [16,41]. The reason for the increase in hardness at SZ is grain size, dislocation density, and presence of hard ceramic nanoparticles.

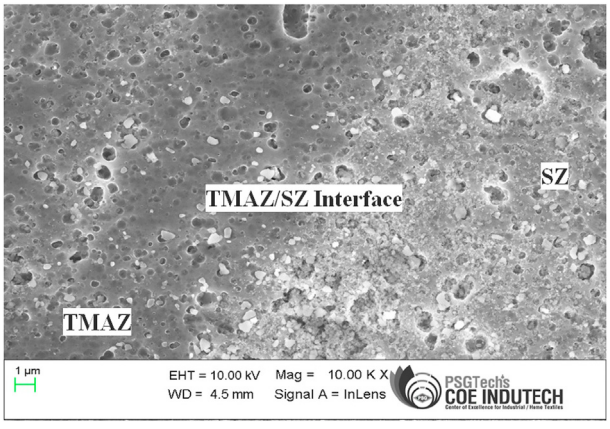

Fig. 12 – FESEM micrograph of TMAZ/SZ Interface of AA6061-T6/SiC FSW Lap joint.

Also evidenced that the microhardness of the advancing side (AS) of SiC added weld joints is higher than the retreating side (RS). This is because of higher temperature and more extrusion of the plasticized material on RS [26]. As a result, more nanoparticles are distributed on RS due to the uneven circulation of deformed plasticized material. TMAZ next to the SZ also shows some improved hardness compared to that of SiC particles-free joint. It means that the addition of the nanoparticles has influenced the microhardness of the TMAZ as evidenced in the FESEM image presented in Fig. 12.

The mean microhardness at SZ of sample with 20 vol% of SiC is 92.5 HV, while SiC particle-free joint has 81.5 HV. While comparing these two, the addition of SiC nanoparticles has significant improvement in microhardness by 14%.

4. Conclusion

The Aluminium alloy 6061-T6/SiC composite lap joints were fabricated with SiC nano particles. The macro and microstructure, lap shear strength, microhardness and fracture behaviors of the joints were investigated. Reinforcement of SiC in lap joints looks the best-suited to meet the modern demands of sheet metal application. The findings of investigations include:

- The optimal volume fraction of SiC and tool rotation speed are 20% and 1500 rpm, respectively, to produce defect-free and high strength lap joints.
- SiC nanoparticles are evidenced in and around the grains of the aluminum matrix in SZ leading to grain growth prevention and providing the maximum shear strength and hardness.
- SiC particles are severely agglomerated at higher loading, irrespective of tool rotation speed. The higher loading results non-uniform distribution of nanoparticles and voids at the interface. It leads weaker joints and sudden premature fracture during tensile loading.
- FSW lap joint with 20 vol% shows a ductile fracture at SZ due to well-dispersed SiC particles and strong cohesion at

Al/SiC interfaces. Whereas, joints with a higher loading (26 vol%) shows a brittle fracture due to aggregation of nanoparticles in SZ and poor bonding between nanoparticles and Al matrix.
- Reduction of grain size and impending dislocation mobility are evidenced in SiC added weld joints. It results a significant improvement in microhardness of the SiC added welds as compared with the SiC free joints.

Ethics declarations

The authors declare that they have no known competing financial interest or personal relationships that could have appeared to influence the work reported in this paper.

Funding

Authors thank the National Aeronautics and Space Administration (NASA) MAIANSE CONNECT for providing funding to SPICES (Scheme for Promoting Indegenous Culture and Ethics among STEM Students) project under NASA Cooperative Agreement #80NSSC22K1427 through which this research was carried out with Navajo Technical University.

Author contributions

SS, EN and RS designed the experiment and SS, and AP performed the experimental work; SN and VK analysed the data; SS, EN contributed to original writing the manuscript; RS and VK contributed to review. All authors read and approved the final manuscript.

Consent to Participate

All authors voluntarily agree to participate in this research study.

Consent for publication

All authors give the permission to the Journal to publish this research study.

Availability of data and materials

All data generated or analyzed during this study are included in this published article.

Declaration of Competing Interest

The authors declare that they have no known competing financial interests or personal relationships that could have appeared to influence the work reported in this paper.

Acknowledgement

Not Applicable.

REFERENCES

[1] Tisza M, Czinege I. Comparative study of the application of steels and aluminium in lightweight production of automotive parts. Int J Light Mater Manuf 2018;1:229–38. https://doi.org/10.1016/j.ijlmm.2018.09.001.
[2] Suresh S, Venkatesan K, Natarajan E. Influence of SiC nanoparticle reinforcement on FSS welded 6061-T6 aluminum alloy. J Nanomater 2018;2018:1–11. https://doi.org/10.1155/2018/7031867.
[3] Zhu L, Li N, Childs PRN. Light-weighting in aerospace component and system design. Propuls Power Res 2018;7:103–19. https://doi.org/10.1016/j.jppr.2018.04.001.
[4] Kayaroganam P, Krishnan V, Natarajan E, Natarajan S, Muthusamy K. Drilling parameters analysis on in-situ Al/B4C/mica hybrid composite and an integrated optimization approach using fuzzy model and non-dominated sorting genetic algorithm. Metals 2021;11. https://doi.org/10.3390/met11122060.
[5] Kang M, Kim C. A review of joining processes for high strength 7 xxx series aluminum alloys. J Weld Join 2017;35. https://doi.org/10.5781/JWJ.2017.35.6.12.
[6] Zhong Z-W. Processes for environmentally friendly and/or cost-effective manufacturing. Mater Manuf Process 2021;36:987–1009. https://doi.org/10.1080/10426914.2021.1885709.
[7] Xiao S, Deng Y, Zeng J, Zhang W, Huang L. Effect of heat input on microstructure and mechanical properties of friction stir welded AA2024 and AA7075 dissimilar alloys. J Mater Eng Perform 2021;30:7989–97. https://doi.org/10.1007/s11665-021-06000-y.
[8] Tao W, Shuwei D, Matsuda K, Yong Z. Dynamic recrystallization and dynamic precipitation in AA6061 aluminum alloy during friction stir welding. Trans Indian Inst Met 2022;75(5):1329–39. https://doi.org/10.1007/s12666-021-02490-5.
[9] Ahmed S, Saha P. Development and testing of fixtures for friction stir welding of thin aluminium sheets. J Mater Process Technol 2018;252:242–8. https://doi.org/10.1016/j.jmatprotec.2017.09.034.
[10] Huang Y, Meng X, Zhang Y, Cao J, Feng J. Micro friction stir welding of ultra-thin Al-6061 sheets. J Mater Process Technol 2017;250:313–9. https://doi.org/10.1016/j.jmatprotec.2017.07.031.
[11] Liu FJ, Fu L, Chen HY. Microstructure evolution and fracture behaviour of friction stir welded 6061-T6 thin plate joints under high rotational speed. Sci Technol Weld Join 2018;23:333–43. https://doi.org/10.1080/13621718.2017.1389837.
[12] Gite RA, Loharkar PK, Shimpi R. Friction stir welding parameters and application: a review. Mater Today Proc 2019;19:361–5. https://doi.org/10.1016/j.matpr.2019.07.613.
[13] Singh VP, Patel SK, Ranjan A, Kuriachen B. Recent research progress in solid state friction-stir welding of aluminium–magnesium alloys: a critical review. J Mater Res Technol 2020;9:6217–56. https://doi.org/10.1016/j.jmrt.2020.01.008.
[14] Suresh S, Venkatesan K, Natarajan E, Rajesh S, Lim WH. Evaluating weld properties of conventional and swept friction stir spot welded 6061-t6 aluminium alloy. Mater Express 2019;9:851–60. https://doi.org/10.1166/mex.2019.1584.

[15] Anton Savio Lewise K, Edwin Raja Dhas J. FSSW process parameter optimization for AA2024 and AA7075 alloy. Mater Manuf Process 2021:1–9. https://doi.org/10.1080/10426914.2021.1962532.
[16] Sudhagar S, Gopal PM. Investigation on mechanical and tribological characteristics Cu/Si3N4 surface composite developed through friction stir processing. Silicon 2021:1–10.
[17] Qiao K, Zhang T, Wang K, Yuan S, Wang L, Chen S, et al. Effect of multi-pass friction stir processing on the microstructure evolution and corrosion behavior of ZrO2/AZ31 magnesium matrix composite. J Mater Res Technol 2022;18:1166–79. https://doi.org/10.1016/j.jmrt.2022.02.127.
[18] Singh T, Tiwari SK, Shukla DK. Effects of Al 2 O 3 nanoparticles volume fractions on microstructural and mechanical characteristics of friction stir welded nanocomposites. Nanocomposites 2020;6:76–84. https://doi.org/10.1080/20550324.2020.1776504.
[19] Suresh S, Venkatesan K, Rajesh S. Optimization of process parameters for friction stir spot welding of AA6061/Al2O3 by Taguchi method. AIP Conf Proc 2019:030018. https://doi.org/10.1063/1.5117961.
[20] Suresh S, Elango N, Venkatesan K, Lim WH, Palanikumar K, Rajesh S. Sustainable friction stir spot welding of 6061-T6 aluminium alloy using improved non-dominated sorting teaching learning algorithm. J Mater Res Technol 2020;9:11650–74. https://doi.org/10.1016/j.jmrt.2020.08.043.
[21] AbuShanab WS, Moustafa EB. Effects of friction stir processing parameters on the wear resistance and mechanical properties of fabricated metal matrix nanocomposites (MMNCs) surface. J Mater Res Technol 2020;9:7460–71. https://doi.org/10.1016/j.jmrt.2020.04.073.
[22] Bharti S, Ghetiya ND, Patel KM. A review on manufacturing the surface composites by friction stir processing. Mater Manuf Process 2021;36:135–70. https://doi.org/10.1080/10426914.2020.1813897.
[23] Suresh S, Venkatesan K, Natarajan E, Rajesh S. Performance analysis of nano silicon carbide reinforced swept friction stir spot weld joint in AA6061-T6 alloy. Silicon 2021;13:3399–412. https://doi.org/10.1007/s12633-020-00751-4.
[24] Jafari H, Mansouri H, Honarpisheh M. Investigation of residual stress distribution of dissimilar Al-7075-T6 and Al-6061-T6 in the friction stir welding process strengthened with SiO2 nanoparticles. J Manuf Process 2019;43:145–53. https://doi.org/10.1016/j.jmapro.2019.05.023.
[25] Singh A, Kumar V, Grover NK. A study of microstructure and mechanical properties of friction stir welding aluminium alloy AA6082 with Zn interlayer. Mater Res Express 2019;6:116596. https://doi.org/10.1088/2053-1591/ab4b1f.
[26] Singh T, Tiwari SK, Shukla DK. Friction-stir welding of AA6061-T6: the effects of Al2O3 nano-particles addition. Results Mater 2019;1:100005. https://doi.org/10.1016/j.rinma.2019.100005.
[27] Bahrami M, Helmi N, Dehghani K, Givi MKB. Exploring the effects of SiC reinforcement incorporation on mechanical properties of friction stir welded 7075 aluminum alloy: fatigue life, impact energy, tensile strength. Mater Sci Eng, A 2014;595:173–8. https://doi.org/10.1016/j.msea.2013.11.068.
[28] Maurya R, Kumar B, Ariharan S, Ramkumar J, Balani K. Effect of carbonaceous reinforcements on the mechanical and tribological properties of friction stir processed Al6061 alloy. Mater Des 2016;98:155–66. https://doi.org/10.1016/j.matdes.2016.03.021.
[29] West M, Jasthi B, Hosemann P, Sodesetti V. Friction stir welding of Oxide dispersion strengthened alloy MA956. Frict. Stir weld. Process. VI. Hoboken, NJ, USA: John Wiley & Sons, Inc.; 2011. p. 33–40. https://doi.org/10.1002/9781118062302.ch5.
[30] Thangarasu A, Murugan N, Dinaharan I, Vijay SJ. Synthesis and characterization of titanium carbide particulate reinforced AA6082 aluminium alloy composites via friction stir processing. Arch Civil Mech Eng 2015;15:324–34. https://doi.org/10.1016/j.acme.2014.05.010.
[31] Suresh S, Venkatesan K, Natarajan E, Rajesh S. Influence of tool rotational speed on the properties of friction stir spot welded AA7075-T6/Al2O3 composite joint. Mater Today Proc 2020;27:62–7. https://doi.org/10.1016/j.matpr.2019.08.220.
[32] Chandran R, Ramaiyan S, Shanbhag AG, Santhanam SKV. Optimization of welding parameters for friction stir lap welding of AA6061-T6 alloy. Mod Mech Eng 2018;8:31–41. https://doi.org/10.4236/mme.2018.81003.
[33] Delgado-Pamanes M, Alvarez-Montufar J, Reyes-Osorio L, Garza C, Suárez-Rosales M, Chávez-Alcalá J. Evaluation of optimal processing parameters for a Zn-based eutectoid alloy processed by friction-stir welding. J Mater Res Technol 2022;18:3256–65. https://doi.org/10.1016/j.jmrt.2022.03.181.
[34] Sachinkumar, Narendranath S, Chakradhar D. Microstructure, hardness and tensile properties of friction stir welded aluminum matrix composite reinforced with SiC and fly ash. Silicon 2019;11:2557–65. https://doi.org/10.1007/s12633-018-0044-5.
[35] Fotoohi Nezhad Khales M, Sajjadi SA, Kamyabi-Gol A. Multipass friction stir processing of steel/SiC nanocomposite: assessment of microstructure and tribological properties. J Mater Eng Perform 2020;29:4241–50. https://doi.org/10.1007/s11665-020-04947-y.
[36] Su H, Gao W, Feng Z, Lu Z. Processing, microstructure and tensile properties of nano-sized Al2O3 particle reinforced aluminum matrix composites. Mater Des 2012;36:590–6. https://doi.org/10.1016/j.matdes.2011.11.064.
[37] Zhang Z, Yang X, Zhang J, Zhou G, Xu X, Zou B. Effect of welding parameters on microstructure and mechanical properties of friction stir spot welded 5052 aluminum alloy. Mater Des 2011;32:4461–70. https://doi.org/10.1016/j.matdes.2011.03.058.
[38] Cartigueyen S, Mahadevan K. Wear characteristics of copper-based surface-level microcomposites and nanocomposites prepared by friction stir processing. Friction 2016;4:39–49. https://doi.org/10.1007/s40544-016-0102-1.
[39] Anil Kumar KS, Murigendrappa SM, Kumar H. Experimental investigation on effects of varying volume fractions of SiC nanoparticle reinforcement on microstructure and mechanical properties in friction-stir-welded dissimilar joints of AA2024-T351 and AA7075-T651. J Mater Res 2019;34:1229–47. https://doi.org/10.1557/jmr.2018.445.
[40] Wang R, Kang H-T, Lei X. Fatigue performance and strength assessment of AA2024 alloy friction stir lap welds. J Mater Eng Perform 2020;29:6701–13. https://doi.org/10.1007/s11665-020-05145-6.
[41] Bagheri B, Mahdian Rizi AA, Abbasi M, Givi M. Friction stir spot vibration welding: improving the microstructure and mechanical properties of Al5083 joint. Metallogr Microstruct Anal 2019;8:713–25. https://doi.org/10.1007/s13632-019-00563-y.